Cell Death and Differentiation (2017) 24, 672–682
Official journal of the Cell Death Differentiation Association
www.nature.com/cdd

OPEN

Loss of menin in osteoblast lineage affects osteocyte–osteoclast crosstalk causing osteoporosis

Peng Liu[1,2], Sooyeon Lee[1,2], Jeanette Knoll[2], Alexander Rauch[2,9], Susanne Ostermay[2], Julia Luther[3], Nicole Malkusch[1], Ulf H Lerner[4], Mario M Zaiss[5], Mona Neven[3], Rainer Wittig[6], Martina Rauner[7], Jean-Pierre David[3,5], Philippe Bertolino[8], Chang X Zhang[8] and Jan P Tuckermann*[,1,2]

During osteoporosis bone formation by osteoblasts is reduced and/or bone resorption by osteoclasts is enhanced. Currently, only a few factors have been identified in the regulation of bone integrity by osteoblast-derived osteocytes. In this study, we show that specific disruption of menin, encoded by *multiple endocrine neoplasia type 1* (*Men1*), in osteoblasts and osteocytes caused osteoporosis despite the preservation of osteoblast differentiation and the bone formation rate. Instead, an increase in osteoclast numbers and bone resorption was detected that persisted even when the deletion of *Men1* was restricted to osteocytes. We demonstrate that isolated *Men1*-deficient osteocytes expressed numerous soluble mediators, such as C-X-C motif chemokine 10 (CXCL10), and that CXCL10-mediated osteoclastogenesis was reduced by CXCL10-neutralizing antibodies. Collectively, our data reveal a novel role for *Men1* in osteocyte–osteoclast crosstalk by controlling osteoclastogenesis through the action of soluble factors. A role for *Men1* in maintaining bone integrity and thereby preventing osteoporosis is proposed.
Cell Death and Differentiation (2017) **24,** 672–682; doi:10.1038/cdd.2016.165; published online 20 January 2017

The maintenance of bone mass is severely affected in osteoporotic patients and other bone disorders and can have multiple etiologies. The complex communication of bone-forming osteoblasts, bone-residing osteocytes, and bone-resorbing osteoclasts is still not fully understood. Two hallmark studies[1,2] have demonstrated that osteocytes are the major source of the osteoclastogenesis-stimulating factor RANKL and thus key components in the control of bone mass. This property goes beyond their previously suggested function of sensing the mechanical loading of bone.[3] PTH[4] and sclerostin[5] have been reported to stimulate osteocytes to support osteoclastogenesis via a RANKL-dependent pathway. High-mobility group box 1 (HMGB1), which is chemotactic to osteoclasts, is enhanced in apoptotic MLO-Y4 cells;[6] however, there is little information on other factors controlling osteoclast activity by osteoblast-derived osteocytes.

The nuclear protein menin encoded by the gene *Men1* (*multiple endocrine neoplasia type 1*) has recently been suggested to control bone mass at higher age through its influence on the differentiation and function of osteoblasts.[7] *In vitro* studies in cell lines and primary osteoblasts derived from 6-month-old mice showed that menin promotes early osteoblast differentiation in committed cells. Knockdown of *Men1* with antisense oligonucleotides lead to enhanced BMP2 signaling[8–10] and to facilitated inhibition of the late stage of osteoblast differentiation by potentiating TGFβ-dependent Smad3 signaling.[11,12] Accordingly, reduced bone mass and reduced bone formation due to decreased osteoblast proliferation and differentiation and enhanced apoptosis have been reported using aged osteocalcin-cre mice crossed to *Men1* floxed mice that leads to a conditional deletion of menin in the late stage of differentiated osteoblasts.[7] On the other hand, aged osteoblast-specific menin transgenic mice were found to display increased bone mass.[7] However, whether *Men1* plays a role in bone cells to control bone integrity in young or middle-aged mice is completely unknown.

Using multiple cre-lines, we comprehensively analyzed the effects of loss of function of menin throughout the osteoblast lineage, in osteoclasts, and in osteocytes on bone integrity. Furthermore, we identified genes under the control of *Men1* responsible for the osteocyte-dependent regulation of osteoclast formation.

Results

Men1 disruption in the osteoblast lineage severely affects bone mass but not the bone formation rate. In order to address the role of *Men1* in the entire osteoblast lineage including osteocytes *in vivo*, we generated mice lacking *Men1* specifically in the osteoblast lineage by

[1]Institute of Comparative Molecular Endocrinology, University of Ulm, Ulm D-89081, Germany; [2]Tissue-specific Hormone Action, Leibniz Institute on Aging–Fritz Lipmann Institute (FLI), Jena D-07745, Germany; [3]Department of Osteology and Biomechanics, University Medical Center Hamburg-Eppendorf, Hamburg D-20246, Germany; [4]Centre for Bone and Arthritis Research, Department of Internal Medicine and Clinical Nutrition at Institute for Medicine, Sahlgrenska Academy at University of Gothenburg, Gothenburg SE-41345, Sweden; [5]Department of Internal Medicine 3-Rheumatology and Immunology, Friedrich-Alexander-University Erlangen-Nürnberg (FAU) and Universitätsklinikum Erlangen, Erlangen D-91054, Germany; [6]Institute for Laser Technologies in Medicine and Metrology at Ulm University, Ulm D-89081, Germany; [7]Division of Endocrinology and Bone Diseases, Department of Medicine III, TU Dresden, Dresden D-01307, Germany and [8]Centre de Recherche en Cancérologie de Lyon, Inserm U1052, CNRS UMR5286, Université Lyon 1, Lyon F-69000, France
*Corresponding author: JP Tuckermann, Institute of Comparative Molecular Endocrinology, University of Ulm, Ulm D-89081, Germany. Tel: +49 731 50 32600; Fax: +49 731 50 32609; E-mail: jan.tuckermann@uni-ulm.de
[9]Current address: Department of Biochemistry and Molecular Biology, University of Southern Denmark, DK-5230 Odense, Denmark.
Received 30.6.16; revised 08.12.16; accepted 20.12.16; Edited by E Wagner; published online 20.1.2017

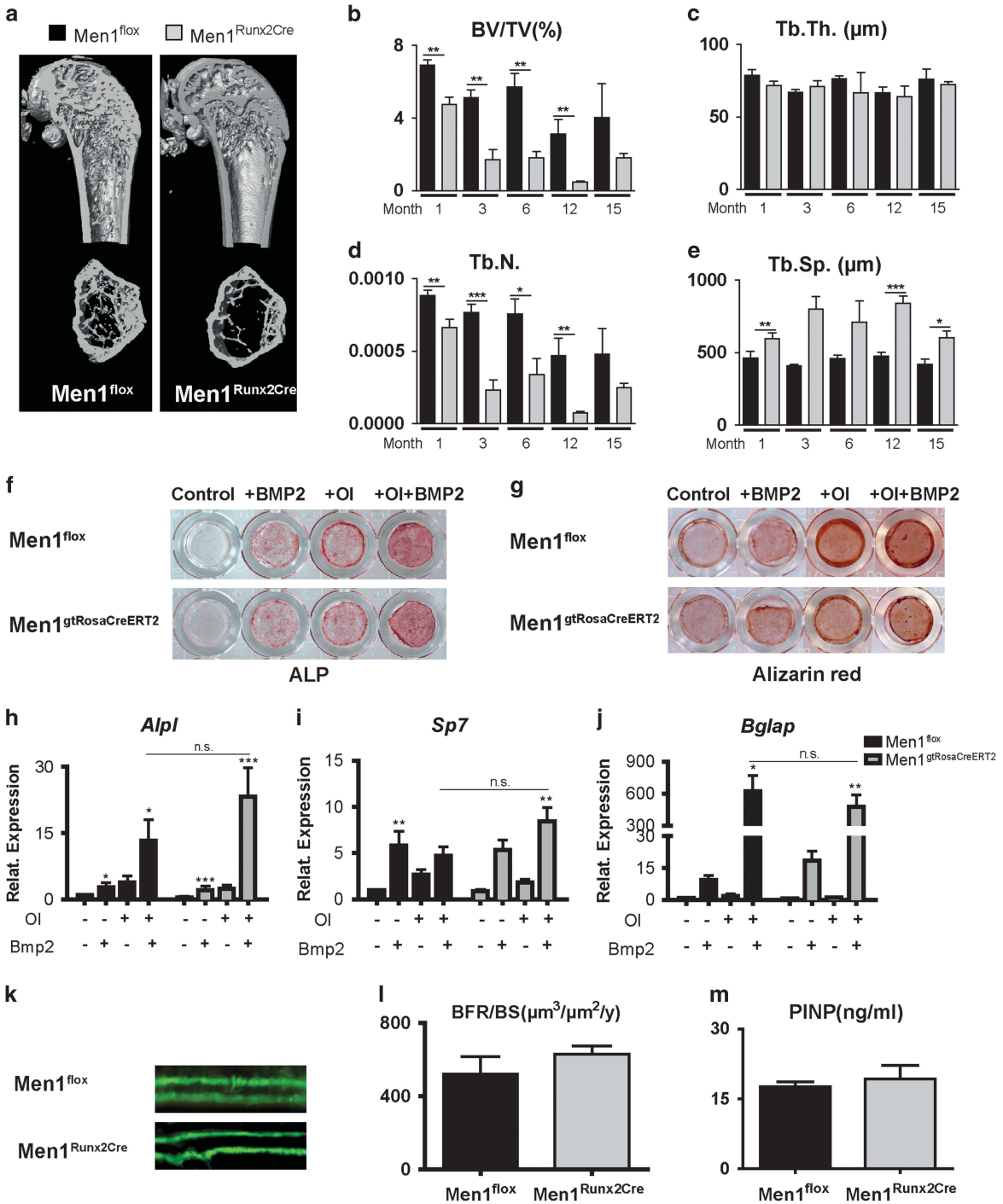

Figure 1 Disrupting *Men1* in the osteoblast lineage causes bone loss without altering the bone formation rate. (**a**) Micro CT reconstruction of femurs from 12-week-old female *Men1*^{flox} and *Men1*^{Runx2Cre} mice. (**b**–**e**) Cancellous parameters such as bone volume per tissue volume (BV/TV) (**b**), trabecular thickness (Tb.Th.) (**c**), trabecular numbers (Tb.N.) (**d**), and trabecular separation (Tb.Sp.) (**e**) were measured from distal femurs of female *Men1*^{flox} and *Men1*^{Runx2Cre} mice at indicated age by micro CT ($n=4$ or 5). $^{*}P<0.05$, $^{**}P<0.01$, $^{***}P<0.001$. (**f** and **g**) Primary calvarial osteoblasts were isolated from *Men1*^{flox} and *Men1*^{gtRosaCreERT2} mice. After pretreatment with 4-OHT to allow recombination of the *Men1*flox allele, cells were cultured with or without osteogenic induction (OI) medium in the absence or presence of BMP2 for 7 and 12 days and stained for alkaline phosphatase (**f**) and alizarin red (**g**), respectively. (**h**–**j**) mRNA expression levels of *Alpl* (**h**) and *Sp7* (**i**) from 7-day-treated cells as in (**f**), and *Bglap* (**j**) from 12-day-treated cells as in (**g**) were analyzed by QRT-PCR ($n=5$). $^{*}P<0.05$, $^{**}P<0.01$, $^{***}P<0.001$ *versus* untreated *Men1*^{flox}. (**k** and **l**) Fluorescent micrographs of dual calcein labeling (**k**) and its quantitative analysis of bone formation rate per bone surface (BFR/BS) (**l**) by dynamic histomorphometry in femurs of 12-week-old female *Men1*^{flox} and *Men1*^{Runx2Cre} mice ($n=4$ or 5). (**m**) Determination of the serum PINP level (a bone formation marker) in 12-week-old female *Men1*^{flox} and *Men1*^{Runx2Cre} mice ($n=5$). Data are represented as mean ± S.E.M.

crossing *Men1*$^{tm1.1Zqw}$ (hereafter designated *Men1*^{flox}) mice[13] to Tg(Runx2-icre)1Jtuc (hereafter designated Runx2Cre) mice[14] to obtain *Men1*^{Runx2Cre} mice. Immunohistochemistry of femurs indicated a decreased menin expression in osteoblasts and osteocytes of *Men1*^{Runx2Cre} mice (Supplementary Figure S1a). Successful recombination was additionally confirmed by crossing a Rosa$^{mT/mG}$ (Tomato/EGFP) reporter mouse[15] to Runx2Cre mice and demonstrating cre-loxP recombination by GFP-positive osteoblasts and osteocytes (Supplementary Figure S1b). *Men1*^{Runx2Cre} mice were viable without gross alterations of the skeleton (Supplementary Figure S1c) and were born slightly below the Mendelian ratio (Supplementary Table S1).

Strikingly, micro computed tomography (micro CT) revealed a strong bone loss in the distal femur of female *Men1*^{Runx2Cre} mice (Figures 1a–e). This bone loss was observed in 4-week-old mice and persisted upon aging (Figures 1b–e). Similarly, bone loss was observed in male *Men1*^{Runx2Cre} mice (Supplementary Table S2), resembling osteoporosis. Although trabecular thickness remained unaltered, the strong decrease of trabecular bone mass in *Men1*^{Runx2Cre} mice was found to be caused by a low number of trabeculae and an increased trabecular separation (Figures 1b–e and Supplementary Table S2). Notably, cortical bone thickness in the femur was unchanged (Supplementary Table S3). Histomorphometry and micro CT analysis of tibiae and vertebrae confirmed the trabecular bone loss (Supplementary Figures S1d–h and Supplementary Table S2). Next, we analyzed whether the osteoporotic phenotype was specifically dependent on the elimination of *Men1* in the osteoblast lineage.

First, we corroborated that the observed bone loss strictly depended on elimination of *Men1* in the osteoblast lineage. Mice with a disruption of *Men1* in the myeloid lineage (Lyz2$^{tm1(cre)Ifo}$,[16] hereafter designated *Men1*^{LysMCre} mice) including osteoclasts (Supplementary Figures S2a and b) did not display any alterations in trabecular bone volume, trabecular thickness, numbers, and separation (Supplementary Figures S2c–f). In contrast, eliminating *Men1* in the early differentiated osteoblast lineage using another osteoblast-specific cre-line, Tg(Sp7-tTA,tetO-EGFP/cre)1Amc (hereafter designated OsxCre) mice,[17] reproduced the severe osteoporosis as observed in *Men1*^{Runx2Cre} mice. The resulting *Men1*^{OsxCre} mice also displayed a strong decrease of trabecular bone volume and trabecular numbers and an increased trabecular separation, whereas trabecular thickness was only slightly affected (Supplementary Table S2).

Second, we asked whether loss of *Men1* influenced the expression of osteoblast marker genes and osteoblast numbers *in vivo*. The mRNA expression of osteoblast marker genes such as *Alpl*, *Col1a1*, *Runx2*, and *Bglap* was similar in the calvarial bone of *Men1*^{Runx2Cre} mice compared with control (*Men1*^{flox}) (Supplementary Figures S3a–d). In line with this, dynamic histomorphometry of vertebrae did not detect significant changes of osteoblast numbers and osteoblast surface (Supplementary Figures S3e and f). Osteocyte number was significantly higher in *Men1*^{Runx2Cre} mice (Supplementary Figure S3g).

Furthermore, we asked whether *Men1* deficiency could influence osteoblast differentiation *in vitro* as suggested in previous studies.[7,12] To eliminate *Men1* efficiently in osteoblast progenitor cells, we cultivated mesenchymal progenitor cells and primary calvarial osteoblasts derived from *Men1*^{flox} mice crossed to a mouse line with ubiquitous expression of a Cre-ERT2 fusion protein (Gt(ROSA)26Sor$^{tm9(Cre/ESR1)Arte}$, hereafter designated gtRosaCreERT2), allowing a dramatic decrease in *Men1* expression upon tamoxifen treatment (Supplementary Figures S3o, p, and s). Disruption of *Men1* *in vitro* did not affect the growth of calvarial osteoblasts (Supplementary Figure S3h). Intriguingly, the differentiation of *Men1*-deficient calvarial osteoblasts and mesenchymal progenitor cells was unaffected and the cells responded normally to BMP2-induced differentiation as indicated by histochemical staining (Figures 1f, g and Supplementary Figures S3i–l) and marker gene expression (Figures 1h–j, Supplementary Figures S3m and n). In accordance with these results, no major differences were observed in the BMP2-induced phosphorylation of Smad1/5/8 (Supplementary Figure S3p) and induction of the BMP2–Smad target genes *Id1* and *Dlx5* (Supplementary Figures S3q and r) between control and *Men1*-deficient cells.

As it was previously reported that inhibiting *Men1* expression with antisense oligonucleotides could affect TGFβ signaling,[11] we also analyzed the TGFβ-induced phosphorylation of Smad3 as well as the expression of TGFβ-induced genes in the absence of *Men1* in osteoblasts. No significant difference was found at the level of Smad3 phosphorylation, nor at expression levels of the TGFβ target genes *Serpine* and *Skil* in the absence of *Men1* (Supplementary Figures S3s–u).

In accordance with the unaltered osteoblast differentiation, there was no difference in the bone formation rate in femurs (Figures 1k and l) and vertebrae (Supplementary Figures S3v and w) of 12-week-old *Men1*^{flox} and *Men1*^{Runx2Cre} mice. Correspondingly, the serum PINP level was not changed in *Men1*^{Runx2Cre} mice (Figure 1m). However, the bone formation rate in 12-month-old *Men1*^{Runx2Cre} mice was significantly reduced (Supplementary Figures S3x and y). This corroborates the finding of Kanazawa *et al*.[7] who described impaired osteoblast function in 9- and 12-month-old mice in which *Men1* was eliminated by an osteocalcin-cre.

In summary, despite a possible role for *Men1* in bone formation during aging, no drastic changes of osteoblast marker gene expression, osteoblast number, and osteoblast function were observed in young and middle-aged mice lacking *Men1* in the osteoblast lineage.

Men1 deficiency in the osteoblast lineage, specifically in osteocytes, leads to an enhanced osteoclastogenesis. We observed a strong increase of osteoclast numbers and surface in femurs (Figures 2a and b) and vertebrae (Supplementary Figures S4a and b). These increases were also seen in calvaria (Supplementary Figures S4c–e) and were associated with a high porosity (Supplementary Figure S4f). Bone resorption as determined by serum C-terminal telopeptide (CTX) level was increased in 12-week-old *Men1*^{Runx2Cre} mice (Figure 2c). To test whether *Men1*-deficient osteoblasts could cause greater osteoclastogenesis, we performed osteoblast–osteoclast co-culture by using control or *Men1*-deficient osteoblasts and wild-type osteoclast precursors. Surprisingly, the *Men1*-deficient

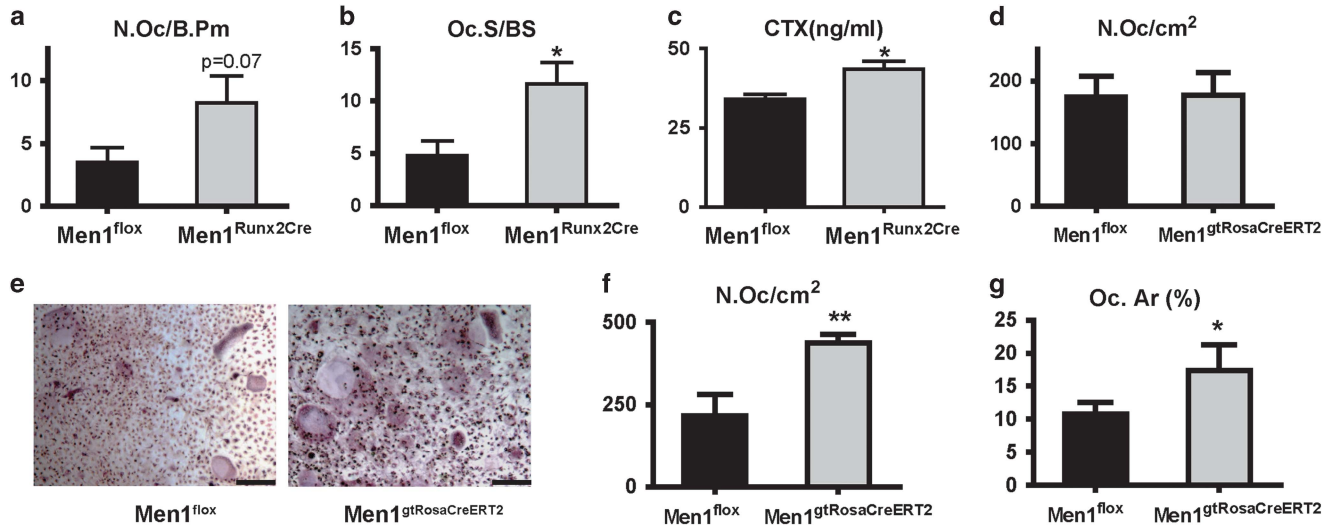

Figure 2 Bone resorption is enhanced in *Men1*^{Runx2Cre} mice, caused by *Men1* deficiency in osteocytes. (**a** and **b**) Osteoclast numbers per bone perimeter (N.Oc/B.Pm) (**a**) and osteoclast surface per bone surface (Oc.S/BS) (**b**) in sections of femoral trabecular bone were measured by histomorphometry ($n=4$ or 5). (**c**) Determination of resorption by assessment of the serum level of the biomarker CTX in 12-week-old female *Men1*^{flox} and *Men1*^{Runx2Cre} mice ($n=5$). (**d**) Number of multinucleated TRAP-positive osteoclasts was counted from primary co-cultures of wild-type BMCs with *Men1*^{flox} or *Men1*^{gtRosaCreERT2} primary osteoblasts ($n=3$). (**e**–**g**) Osteoclastogenesis of primary co-cultures of wild-type BMCs with *Men1*^{flox} or *Men1*^{gtRosaCreERT2} primary osteocytes was visualized by TRAP staining (**e**). Number of multinucleated TRAP-positive cells (**f**) and their area (**g**) were determined ($n=3$). $^{*}P<0.05$, $^{**}P<0.01$. Data are represented as mean ± S.E.M. Scale bar: 25 μm

osteoblasts could not trigger higher osteoclast numbers (Figure 2d).

Osteocytes were recently established as major producers of RANKL in bone and therefore important regulators of osteoclastogenesis.[1,2] As deletion of *Men1* by the cre-loxP system in osteoblasts also affects *Men1* expression in osteocytes (Supplementary Figures S1a and b), we further tested the capacity of *Men1*-deficient osteocytes to stimulate osteoclast formation *ex vivo*. To this end, we isolated primary osteocyte-enriched fractions from *Men1*^{gtRosaCreERT2} mice. These cells expressed higher *Dmp1* and lower *Alpl* levels when compared with primary osteoblasts, confirming the efficacy of the isolation of osteocytes (Supplementary Figures S5a and b). Following 4-hydroxytamoxifen (4-OHT) treatment to eliminate the *Men1* gene (Supplementary Figure S5c), the osteocyte-enriched fraction was co-cultivated with wild-type bone marrow cells (BMCs) containing osteoclast progenitor cells. As a result, osteoclast number and osteoclast area were significantly higher in the co-culture containing *Men1*-deficient osteocytes (Figures 2e–g).

Men1 deficiency in osteocytes leads to an enhanced osteoclastogenesis *in vivo*. The *in vitro* co-culture experiments suggested that the increased osteoclast number in the mice lacking *Men1* in the osteoblastic lineage was conferred by *Men1*-deficient osteocytes rather than osteoblasts. To confirm this hypothesis *in vivo*, we generated mice lacking *Men1* in osteocytes, but not in early differentiated osteoblasts, by crossing *Men1*^{flox} mice to Tg(Dmp1-cre)1Jqfe (hereafter designated Dmp1Cre) mice[18] to obtain *Men1*^{Dmp1Cre} mice. Loss of menin in osteocytes in *Men1*^{Dmp1Cre} mice was confirmed by immunohistochemistry (Supplementary Figure S5d) and by crossing *Men1*^{Dmp1Cre} mice to Rosa$^{mT/mG}$ reporter mice that displayed a strongly diminished *Men1* expression in GFP-positive cells (Figure 3a and Supplementary Figure S5e). As Dmp1 is also expressed in mature osteoblasts, we stained osteocalcin as a mature osteoblast marker in *Men1*^{Dmp1Cre}; Rosa$^{mT/mG}$ reporter mice (Supplementary Figure S5f) to determine the degree of recombination in these cells. We found that 29 ± 9% of osteocalcin-stained mature osteoblasts were EGFP positive, indicating that a minor fraction of the late-stage differentiated osteoblasts is also mutant in addition to osteocytes in *Men1*^{Dmp1Cre}; Rosa$^{mT/mG}$ mice. Micro CT analysis revealed a severe osteoporosis in the distal femur of adult *Men1*^{Dmp1Cre} mice (Figures 3b–f). The decrease of trabecular bone mass in *Men1*^{Dmp1Cre} mice was because of a low number of trabeculae and an increased trabecular separation. Trabecular thickness was again unchanged. Osteoblast number, osteoblast surface, and osteocyte number were not altered in *Men1*^{Dmp1Cre} mice (Figures 3g–i). Accordingly, the bone formation rate and serum PINP level were not different between *Men1*^{flox} mice and *Men1*^{Dmp1Cre} mice (Figures 3j–l). Osteoclast number, osteoclast surface, and CTX level were significantly elevated in *Men1*^{Dmp1Cre} mice (Figures 3m–o), whereas RANKL and OPG levels were not changed (Supplementary Figures S5g and h). Thus, a similar bone phenotype was observed in *Men1*^{Dmp1Cre} mice as shown in *Men1*^{Runx2Cre} and *Men1*^{OsxCre} mice. Together with the observed increase of osteoclastogenesis by osteocytes, these observations strongly suggest that osteoporosis by loss of *Men1* is executed by osteocytes in these three different conditional knockout mouse strains.

Menin suppresses CXCL10 to regulate osteocyte–osteoclast crosstalk. We could not detect differences in *Tnfsf11* (RANKL) and *Tnfrsf11b* (OPG) expression in the bone of *Men1*^{Dmp1Cre} mice (Supplementary Figures S6a and b). We

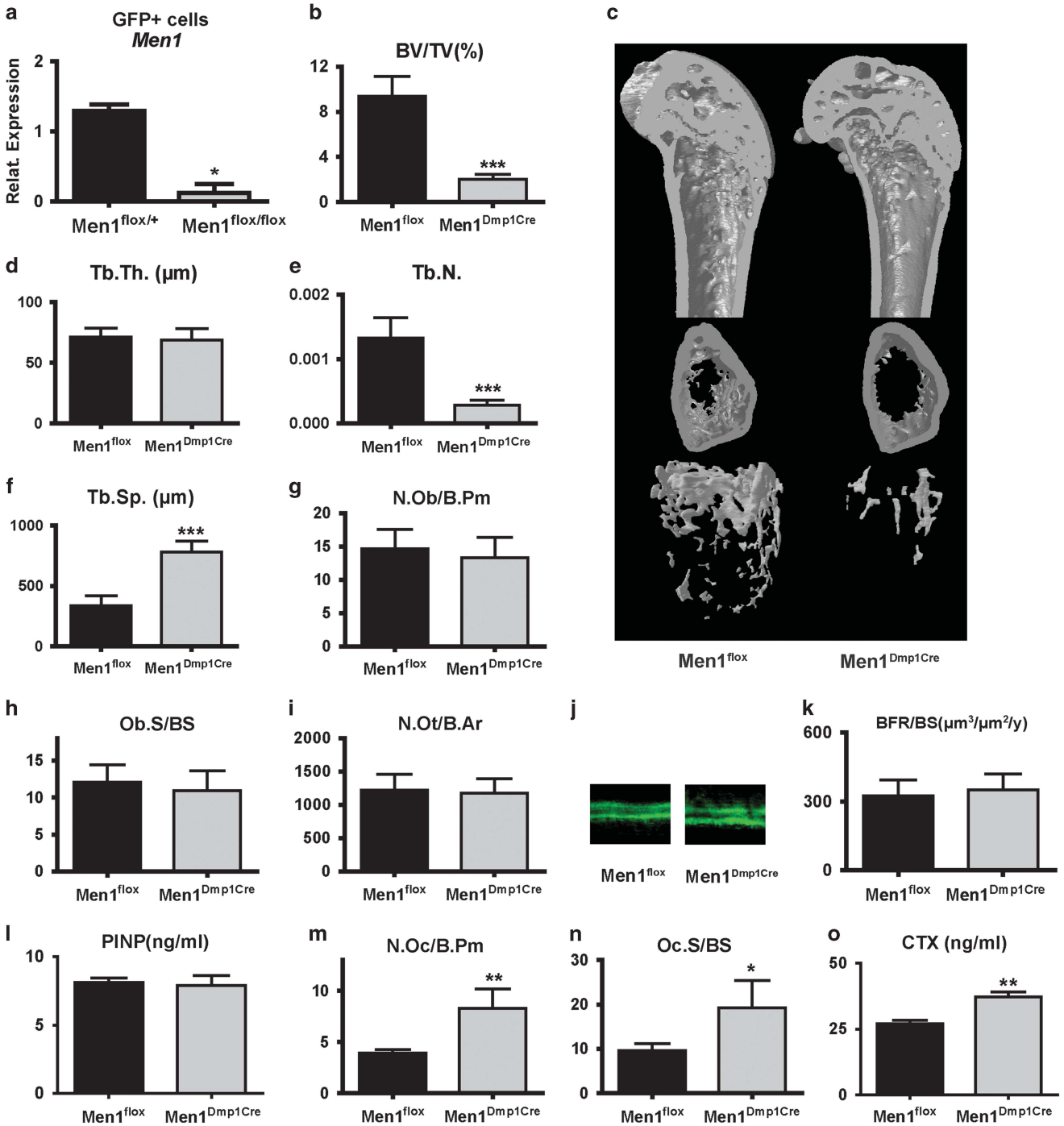

Figure 3 *Men1* deficiency in osteocytes leads to an enhanced osteoclastogenesis *in vivo*. (**a**) Real-time PCR analysis of *Men1* mRNA expression in FACS-sorted GFP-positive cells from femoral bone of *Men1*^{Dmp1Cre} mice crossed to Rosa$^{mT/mG}$ mice in animals heterozygous and homozygous for *Men1*flox. (**b**–**f**) Micro CT reconstruction (**c**) of femurs from 12-week-old female *Men1*^{flox} and *Men1*^{Dmp1Cre} mice. Cancellous parameters such as BV/TV (**b**), Tb.Th. (**d**), Tb.N. (**e**), and Tb.Sp. (**f**) were measured from distal femurs of 12-week-old female *Men1*^{flox} and *Men1*^{Dmp1Cre} mice by micro CT ($n=4$ or 5). (**g**–**i**) Osteoblast number per bone perimeter (N.Ob/B.Pm) (**g**), osteoblast surface per bone surface (Ob.S/BS) (**h**), and osteocyte number per bone area (N.Ot/B.Ar) (**i**) in trabecular bone of distal femoral sections from 12-week-old female *Men1*^{flox} and *Men1*^{Dmp1Cre} mice were measured by histomorphometry ($n=4$ or 5). (**j** and **k**) Fluorescent micrographs of dual calcein labeling (**j**) and its quantitative analysis of BFR/BS (**k**) in femoral sections of 12-week-old female *Men1*^{flox} and *Men1*^{Dmp1Cre} mice ($n=4$ or 5). (**l**) Determination of the serum PINP level in 12-week-old female *Men1*^{flox} and *Men1*^{Dmp1Cre} mice ($n=5$). (**m** and **n**) N.Oc/B.Pm (**m**) and Oc.S/BS (**n**) in trabecular bone of distal femoral sections from 12-week-old female *Men1*^{flox} and *Men1*^{Dmp1Cre} mice were measured by histomorphometry ($n=4$ or 5). (**o**) Determination of resorption from the serum CTX level in 12-week-old female *Men1*^{flox} and *Men1*^{Dmp1Cre} mice ($n=5$). $^{*}P<0.05$, $^{**}P<0.01$, $^{***}P<0.001$. Data are represented as mean ± S.E.M.

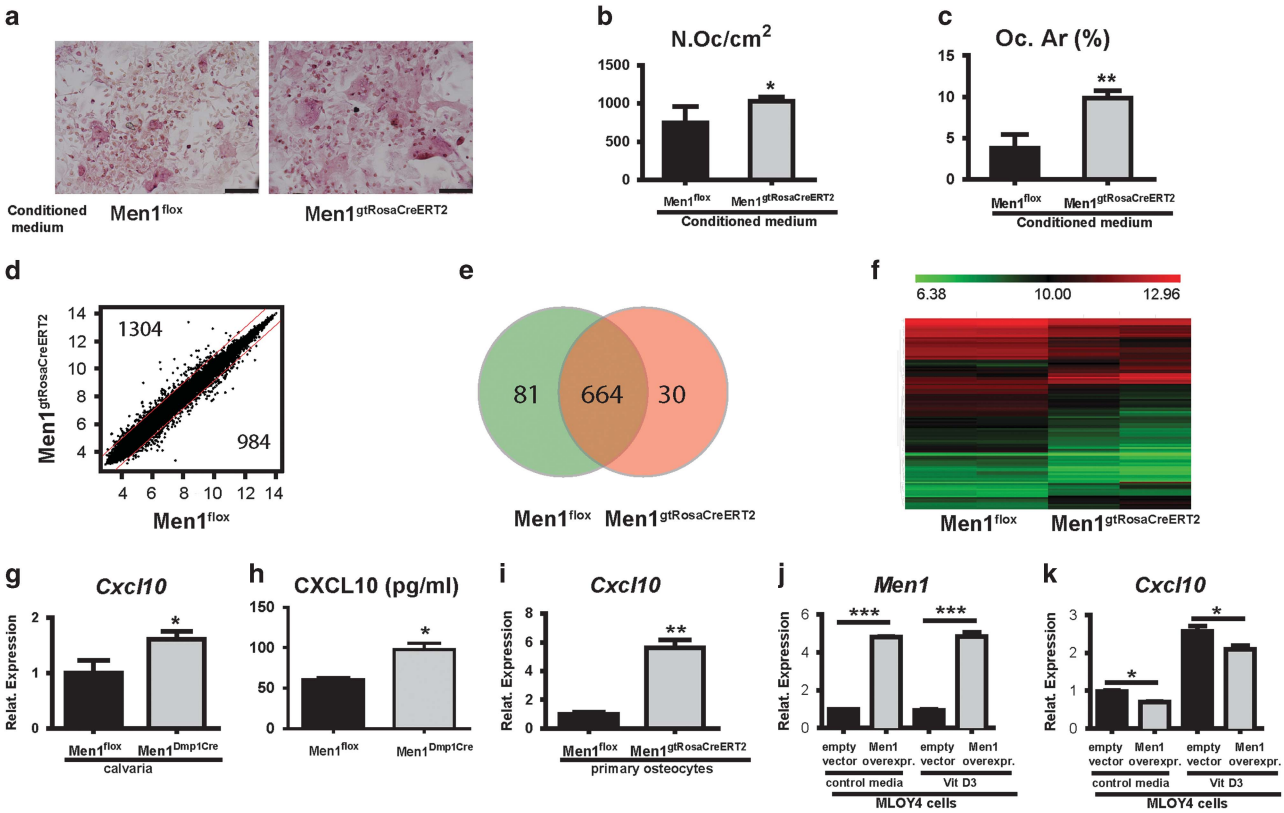

Figure 4 *Men1* deficiency in osteocytes leads to an enhanced osteoclastogenesis via increased *Cxcl10* expression. (**a**–**c**) Osteoclastogenesis was visualized by TRAP staining of co-cultures of primary wild-type osteocytes and BMCs supplemented with conditioned medium from 4-OHT-pretreated $Men1^{flox}$ or $Men1^{gtRosaCreERT2}$ osteocyte cultures (**a**). Number of multinucleated TRAP-positive cells (**b**) and their area (**c**) were determined ($n=3$). (**d**–**f**) Microarray analysis of *Men1*-deficient enriched osteocyte fractions. (**d**) Scatter plot of normalized expression levels of control ($Men1^{flox}$, x axis) and *Men1*-deficient ($Men1^{gtRosaCreERT2}$, y axis) enriched osteocyte fractions. Probe sets outside of the two diagonal lines represent 1.4-fold upregulated or 0.7-fold downregulated genes in *Men1*-deficient cells compared with $Men1^{flox}$ control cells. (**e**) Venn diagram of *Men1*-regulated genes annotated as 'secreted' by DAVID. Numbers indicate genes highly expressed in $Men1^{flox}$ cells (left), no change (middle), or highly expressed in $Men1^{gtRosaCreERT2}$ cells (right), respectively. (**f**) Heat map of normalized expression levels of control (WT, $Men1^{flox}$) and *Men1*-deficient (KO, $Men1^{gtRosaCreERT2}$) osteocytes. Secreted factors with high expression levels ($>50\%$ of the total probe signals) with fold change values ($2^{\text{expression levels (KO-WT)}}$) of >1.4 (30 gene data sets) or <0.7 (81 gene data sets) were visualized in the heat map. (**g**) mRNA levels of *Cxcl10* were determined from calvarial bone of 3-day-old $Men1^{flox}$ and $Men1^{Dmp1Cre}$ mice by QRT-PCR ($n=4$ or 5). (**h**) CXCL10 levels in the supernatant after 5 days of organ culturing of calvaria from neonatal $Men1^{Dmp1Cre}$ mice were determined by ELISA ($n=3$ or 4). (**i**) mRNA levels of *Cxcl10* were determined by QRT-PCR in 4-OHT-pretreated enriched osteocyte fractions isolated from $Men1^{flox}$ and $Men1^{gtRosaCreERT2}$ mice ($n=3$). (**j** and **k**) mRNA levels of *Men1* (**j**) and *Cxcl10* (**k**) were determined by QRT-PCR in *Men1*-overexpressing MLO-Y4 cells after treatment with control media or vitamin D3 ($n=3$). $^*P<0.05$, $^{**}P<0.01$, $^{***}P<0.001$. Data are represented as mean ± S.E.M. Scale bar: 25 μm

therefore tested whether other soluble factors derived from *Men1*-deficient osteocytes affected osteoclastogenesis. Transfer of conditioned medium from cultured *Men1*-deficient osteocyte-enriched fractions to wild-type osteocyte-enriched fractions/osteoclast co-cultures revealed a higher osteoclast formation than the transfer of medium from wild-type osteocyte-enriched fractions (Figures 4a–c). Furthermore, the conditioned medium from osteocyte-enriched fractions was added to wild-type osteoclast cultures. Again, the conditioned medium from *Men1*-deficient osteocyte-enriched fractions triggered higher osteoclast formation than the medium from control osteocyte-enriched fractions (Supplementary Figures S6c–e).

Our findings from the transfer of conditioned medium suggested that the presence of soluble factors derived from osteocytes lacking *Men1* influenced osteoclastogenesis. Subsequently, we performed a microarray analysis with the mRNA of osteocyte-enriched fractions (Figures 4d–f). In total, 2288 differentially expressed genes were found (Figure 4d). Of these, 775 genes (Figure 4e) were annotated as secreted factors analyzed by DAVID bioinformatics resources.[19] Of the 775 genes, 81 were upregulated in wild-type osteocytes and 30 were more highly expressed in *Men1*-deficient osteocyte-enriched fractions (Figure 4f, e and Supplementary Table S4). Among these 111 genes, 12 were related to osteoclastogenesis based on the literature. All of the 12 osteoclastogenesis-associated genes were subsequently analyzed for their expression in entire calvarial bone of $Men1^{Dmp1Cre}$ mice by QRT-PCR (Figure 4g and Supplementary Figures S6f–p). Of these genes, C-X-C motif chemokine 10 (CXCL10), a previously described osteoclastogenesis-inducing factor,[20] showed the most strikingly elevated expression in entire calvarial bone of $Men1^{Dmp1Cre}$ mice (Figure 4g). We also detected enhanced CXCL10 secretion in supernatant medium of organ cultures of calvarial bones (Figure 4h). Real-time PCR confirmed a significantly higher *Cxcl10* expression in *Men1*-

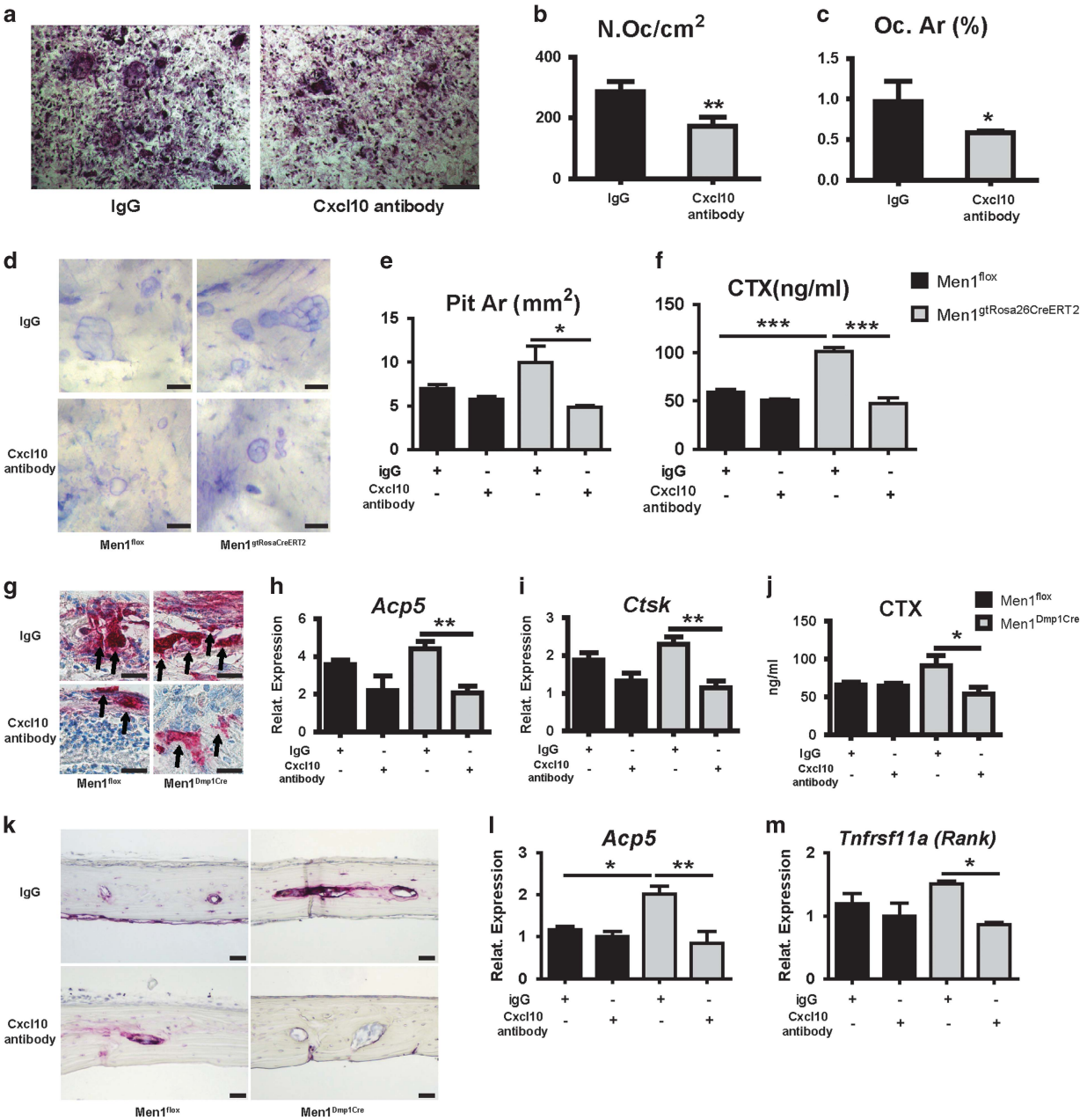

Figure 5 CXCL10-neutralizing antibody rescues enhanced osteoclastogenesis. (**a**–**c**) CXCL10-neutralizing antibody (20 ng/ml) or IgG was added to co-cultures of wild-type BMCs with *Men1*-deficient primary osteocytes isolated from *Men1*^{gtRosaCreERT2} mice and treated with 4-OHT. Co-cultures were stained for TRAP activity (**a**). Number of multinucleated TRAP-positive cells (**b**) and their area (**c**) were determined ($n=3$). (**d**–**f**) CXCL10-neutralizing antibody (20 ng/ml) or IgG was added to co-cultures of wild-type BMCs with primary osteocytes isolated from *Men1*^{flox} and *Men1*^{gtRosaCreERT2} mice and treated with 4-OHT. The co-cultures were seeded on bone slices. Resorption pits were stained with toluidine blue (**d**). Pit area (**e**) and CTX levels in the supernatant (**f**) were determined ($n=3$). (**g**–**j**) Organ cultures of calvaria from neonatal *Men1*^{Dmp1Cre} mice were treated with IgG or CXCL10-neutralizing antibody. TRAP staining was performed and osteoclasts were visualized (arrows) (**g**). *Acp5* (**h**) and *Ctsk* (**i**) mRNA levels were determined by QRT-PCR. CTX levels in the supernatant (**j**) were determined by ELISA ($n=3$ or 4). (**k**–**m**) IgG or CXCL10-neutralizing antibody was subcutaneously injected over the calvaria of 12-week-old female *Men1*^{flox} and *Men1*^{Dmp1Cre} mice. TRAP staining was performed (**k**). *Acp5* (**l**) and *Tnfrsf11a* (**m**) mRNA levels were determined by QRT-PCR ($n=4$). $^{*}P<0.05$, $^{**}P<0.01$, $^{***}P<0.001$. Data are represented as mean ± S.E.M. Scale bar: 25 μm

deficient primary osteocytes (Figure 4i). Similar results were found from calvaria of *Men1*^{Runx2Cre} mice (Supplementary Figure S6q). Contra to the increased *Cxcl10* expression in *Men1*-deficient osteocyte-enriched fractions, *Men1* overexpression in the MLO-Y4 osteocyte cell line (Figure 4j) significantly diminished basal and 1,25-dihydroxyvitamin D3-induced levels of *Cxcl10* expression (Figure 4k). These data indicate a specific role for *Men1* in osteocytes in the regulation of *Cxcl10* expression. Furthermore, CXCL10-neutralizing antibodies significantly reduced osteoclastogenesis in wild-type BMCs co-cultured with *Men1*-deficient osteocyte-enriched fractions (Figures 5a–c). Of note, these

neutralizing antibodies did not affect wild-type osteocyte-enriched fractions co-cultured with BMCs (Supplementary Figures S6r and s). In order to assess the resorption ability *in vitro*, the co-cultures were performed on bone slices. Co-cultures with *Men1*-deficient osteocyte-enriched fractions displayed a clear tendency of higher resorption pit area and significantly increased CTX release that were significantly reduced by the CXCL10-neutralizing antibodies (Figures 5d–f).

We verified these findings in organ cultures of calvaria derived from *Men1*^{Dmp1Cre} mice. TRAP staining, osteoclast marker expression, and the level of resorption marker CTX in the supernatant were all decreased upon CXCL10-neutralizing antibody treatment (Figures 5g–j), indicating that CXCL10 mediates increased osteoclastogenesis and resorption in intact bones.

Furthermore, CXCL10-neutralizing antibodies were subcutaneously injected over the calvaria of *Men1*^{flox} and *Men1*^{Dmp1Cre} mice. Osteoclast indicating TRAP staining was reduced in CXCL10-neutralizing antibody-treated *Men1*^{Dmp1Cre} mice (Figure 5k). Osteoclast marker expression was also reduced in the calvaria of these mice (Figures 5l and m). Thus, these data demonstrate the reduction of enhanced osteoclastogenesis in *Men1*^{Dmp1Cre} mice by CXCL10-neutralizing antibodies *in vivo*.

In summary, *Men1* deficiency specifically in osteocytes increases *Cxcl10* expression and enhances osteoclastogenesis *in vitro* and *in vivo* that contributes to the osteoporotic phenotype observed in mice with a disruption of *Men1* in osteoblast-derived osteocytes (*Men1*^{Runx2Cre}, *Men1*^{OsxCre}, and *Men1*^{Dmp1Cre} mice).

Discussion

In this study, we uncover the role of *Men1* in maintaining bone integrity via osteocyte–osteoclast crosstalk. *Men1* deficiency in the osteoblast lineage does not affect bone formation, whereby *Men1* deficiency in osteocytes promoted osteoclastogenesis by enhancing the production of soluble factors, such as CXCL10, causing osteoporosis in young or middle-aged mice.

In agreement with a previous study,[7] we observed a decrease of bone formation in aged 12-month-old female mice. Strikingly, in middle-aged mice, we unequivocally show that selective *Men1* deletion in the osteoblastic lineage in three distinct conditional *Men1* mutant mouse lines does not alter bone formation, as indicated by the bone formation rate in femurs and vertebrae as well as systemic PINP levels. Our conclusion is supported by the *ex vivo* analysis of osteoblast differentiation in the absence of *Men1* in uncommitted mesenchymal stromal cells and neonatal calvarial osteoblasts. In primary uncommitted mesenchymal stromal cells from 6- to 8-week-old mice and neonatal calvarial osteoblasts from 3- to 5-day-old newborn mice with an efficient deletion of *Men1* using an inducible cre-loxP system, we did not detect any differences in osteoblast proliferation and their differentiation potential. This is in contrast to previous studies by Kanazawa *et al*.[7] who described a decreased osteoblast differentiation of primary calvarial cells derived from 6-month-old *Men1*flox-osteocalcin-cre mice. In addition, previous studies suggested a decrease of BMP2-Smad1/5/8 signaling and an increase of TGFβ signaling upon abrogation of *Men1*.[7,11,12] In osteoblast progenitor cells with a complete elimination of *Men1*, no major difference was evident in either Smad1/5/8 phosphorylation or Smad3 phosphorylation upon BMP2 and TGFβ stimulation, respectively. Furthermore, the response of BMP2 and TGFβ target genes was unaltered and, importantly, the effect on osteoblast differentiation was unchanged in calvarial and mesenchymal stromal cells. These discrepancies may be explained in part by the fact that antisense oligonucleotides were used in the *in vitro* studies,[7,11,12] a technology associated with many undefined off-target effects. The primary cells analyzed by Kanazawa *et al*.[7] were derived from aged calvaria and we cannot exclude the possibility that such old cells devoid of *Men1* display a different response. In summary, our findings support the lack of alterations in osteoblast numbers and the bone formation rate seen in 3-month-old *Men1*^{Runx2Cre} mice *in vivo*.

In this study, we show a novel role for *Men1* in osteocytes governing bone resorption. Osteocytes were recently identified as the major source of RANKL in adult mice that is essential for bone resorption.[1,2] We found in the absence of *Men1* in osteoblasts an increased osteocyte number that was also observed in *Men1*flox-osteocalcin-cre mice.[7] However, in *Men1*^{Dmp1Cre} mice, osteocyte numbers were unaltered, indicating that *Men1* within osteocytes does not affect the abundance of these cells. Nonetheless, in *Men1*^{Dmp1Cre} mice, despite unaltered RANKL expression, we also observed enhanced osteoclast numbers and enhanced resorption based on increased CTX levels in the serum and co-cultures of *Men1*-deficient osteocyte-enriched fractions with osteoclasts. Given that bone mass is already substantially reduced, the elevated levels of CTX indicate a massive enhanced resorption activity in the remaining bone. This was not due to an intrinsic effect of *Men1* in osteoclasts, as there is no recombination in osteoclasts in Runx2Cre,[14] OsxCre,[17] and Dmp1Cre mice.[18] Accordingly, *Men1*^{LysMCre} mice exhibiting a loss of *Men1* in myeloid cells displayed a normal bone phenotype, confirming that bone mass is not affected by *Men1* in osteoclasts.

However, because of the fact that Dmp1Cre recombination occurs in osteocytes as well as in $29 \pm 9\%$ of late-stage osteoblast populations[1] (Supplementary Figure S5f), we cannot fully exclude a possible contribution of *Men1*-deficient osteoblasts to the enhanced osteoclastogenesis. However, the failure of *Men1*-deficient osteoblasts, in contrast to *Men1*-deficient osteocyte-enriched fractions, in enhancing osteoclastogenesis and resorptive activity in co-cultures favors a dominant role of *Men1* in osteocytes in suppressing osteoclastogenesis *in vivo*.

This is further supported by enhanced release of several soluble factors from *Men1*-deficient osteocytes as being a causative determinant for enhanced osteoclastogenesis. For example, conditioned medium derived from *Men1*-deficient osteocyte-enriched fractions displayed an enhanced osteoclastogenic potential, revealing for the first time the role of osteocyte-secreted factors in causing greater osteoclastogenesis. The annotation toward secreted factors from an RNA expression profile defined a potential secretome containing candidate genes important for osteocyte–osteoclast crosstalk

beyond the regulation of RANKL. Among those identified, CXCL10 was found as most strongly induced in entire bone because of a dramatic upregulation found in enriched osteocyte fractions. CXCL10 has been reported to stimulate osteoclast differentiation.[20] Furthermore, the menin-interacting partner MLL regulates *Cxcl10* expression in macrophages and this effect can be abrogated using an MLL–menin inhibitor.[21] We found a clear negative regulation of *Cxcl10* expression by *Men1*, as it was elevated in primary osteocytes and bones from *Men1*^{Dmp1Cre} mice and *Men1*^{Runx2Cre} mice and reduced in *Men1*-overexpressing MLO-Y4 osteocyte cells. The functional relevance of enhanced *Cxcl10* expression was demonstrated by CXCL10-neutralizing antibody treatment of (1) co-cultures, (2) calvarial organ cultures, and (3) mice that resulted in decreased osteoclast formation and resorption as indicated by decreased TRAP staining, osteoclast marker gene expression, and CTX levels. Our data underscore a crucial role of menin in the negative regulation of *Cxcl10* transcription that could be, at least partially, the molecular basis of the enhanced osteoclastogenesis triggered by *Men1* disruption in osteocytes. Given that MDX-1100, an antibody against CXCL10, is in clinical trial phase II for treatment of arthritic patients,[22] this may prove to be an attractive agent to improve bone quality.

Despite the general role of *Men1* in bone integrity, *Men1* conditional knockout mice allow the elucidation of the intrinsic consequences of loss of *MEN1* that might occur in patients suffering from MEN1. The osteopenic phenotype of these patients may be masked by their PTH oversecretion. Intriguingly, following parathyroidectomy, bone recovery is worse in MEN1 patients than in other hyperparathyroidism conditions.[23] Our findings will encourage future analyses on possible mutations in the osteoblastic lineage of MEN1 patients that will enable the PTH effects and osteocyte cell-autonomic effects on bone integrity to be distinguished.

In conclusion, we have established a novel regulatory axis of osteocyte–osteoclast crosstalk regulated by the tumor suppressor gene *Men1*. *Men1* acts in osteocytes to protect trabecular bone mass by modulation of osteoclast function. A *Men1*-regulated chemokine, CXCL10, was identified as an osteocyte–osteoclast crosstalk factor. Modulating *Men1*-regulated factors in osteocytes might serve as a novel molecular base to develop therapeutic strategies to treat osteoporosis.

Materials and Methods

Mice. All mice were kept under standardized conditions with water and food *ad libitum* in specialized pathogen-free animal facilities at the University of Ulm. Procedures for performing animal experiments were in accordance with and approved by the authorities for ethical permission (the Regierungspräsidium in Tübingen, Germany). *Men1*^{Runx2Cre}, *Men1*^{OsxCre}, *Men1*^{gtRosaCreERT2}, *Men1*^{LysMCre}, *Men1*^{Dmp1Cre}, *Men1*^{Dmp1Cre} × Rosa$^{mT/mG}$, and Runx2Cre × Rosa$^{mT/mG}$ mice were generated by intercrossing *Men1*^{flox} mice[13] with Tg(Runx2-icre)1Jtuc mice,[14] Tg (Sp7-tTA,tetO-EGFP/cre)1Amc mice,[17] C57BL/6-Gt(ROSA)26Sor$^{tm9(Cre/ESR1)Arte}$ mice (Taconic Artemis, Köln, Germany), Lyz2$^{tm1(cre)Ifo}$ mice,[16] Tg(Dmp1-cre)1Jqfe mice,[18] and Gt(ROSA)26Sortm4(ACTB-tdTomato,-EGFP)Luo/J mice,[15], respectively

Micro computed tomography. Femurs, tibiae, and lumbar vertebrae were analyzed using a SkyScan 1174 compact micro CT or SkyScan 1176 *in vivo* micro CT (Bruker, Billerica, MA, USA) equipped with an X-ray tube working at 50–80 kV/100 μA. Resolution was 6–9 μm, rotation step was set at 0.40° or 1°, and a 0.5 mm aluminum filter was used. For reconstruction of femurs, the region of interest was defined 0.3 mm from the distal growth plate into the diaphysis spanning 1.8 mm. Trabecular bone volume/tissue volume (BV/TV), trabecular thickness (Tb.Th.), trabecular separation (Tb.Sp.), trabecular number (Tb.N.), cortical thickness (Cs.Th.), cortical closed porosity, and cortical bone perimeter (B.Pm.) were determined according to the guidelines issued by the ASBMR Histomorphometry Nomenclature Committee.[24,25]

Histomorphometry. Static and dynamic histomorphometry was performed on undecalcified and decalcified lumbar vertebral and femoral sections of mice receiving dual calcein (Sigma-Aldrich, St. Louis, MO, USA) i.p. injections, as described previously.[25,26] Osteomeasure software was used for analysis (Osteometrics, Decatur, GA, USA).

Osteoblast differentiation from stromal and calvarial cells. Stromal cells were isolated from inguinal white adipose tissue of *Men1*^{gtRosaCreERT2} mice (6–8 weeks) by digestions for 30 min at 37 °C in isolation buffer containing 100 mM HEPES (Sigma-Aldrich), 120 mM NaCl (Merck, Darmstadt, Germany), 4.8 mM KCl (Sigma-Aldrich), 1 mM $CaCl_2 \bullet 2H_2O$ (Sigma-Aldrich), 4.5 mM glucose (Merck), 1.5% albumin (Sigma-Aldrich), and 0.2% collagenase II (Roche, Rotkreuz, Switzerland). The stromal vascular fraction was collected after filtration and centrifugation and subsequently cultivated as described for calvarial cells below.

Bone marrow stromal cells were isolated from femur and tibia of *Men1*^{gtRosaCreERT2} mice (6–8 weeks). Bone marrows were flushed out and cells were seeded at a density of 1×10^6 cells per cm^2. After 72 h, cells were washed three times with medium (DMEM containing 20% fetal bovine serum and 1% penicillin/streptomycin) and subsequently cultivated as described for calvarial cells below.

Primary osteoblasts isolated from calvaria of neonatal *Men1*^{gtRosaCreERT2} mice (postnatal days 3–5) by sequential digestions were cultivated as previously described.[14] The cells were exposed to 1 μM 4-OHT (Sigma-Aldrich) for 3 days and subsequently subjected to osteogenic induction medium (α-MEM containing 10% fetal bovine serum and 1% penicillin/streptomycin, supplemented with 100 mg/ml sodium ascorbate and 5 mM β-glycerophosphate; Sigma-Aldrich) and/or 100 ng/ml hBMP2 (R&D Systems, Minneapolis, MN, USA). Osteoblast differentiation was determined by alkaline phosphatase and alizarin red (both from Sigma-Aldrich) staining at indicated time points.

Osteoclast differentiation. BMCs were isolated from femurs of 2- to 3-month-old mice and 200 000 cells (diameter >5 μm) were seeded per well in 96-well plates. Differentiation of osteoclasts was performed in α-MEM containing 10% fetal bovine serum and 1% penicillin/streptomycin, supplemented with 50 ng/ml RANKL (PeproTech, Rocky Hill, NJ, USA) and 20 ng/ml M-CSF (R&D Systems) for 5 or 7 days, with the medium changed every 2 or 3 days. TRAP staining was performed using a TRAP-kit (Sigma-Aldrich) and TRAP-positive cells with more than three nuclei were counted as osteoclasts. Osteoclast area was quantified using Osteomeasure software.

For conditioned medium-transfer experiments, conditioned medium from *Men1*-deficient primary osteocyte-enriched fractions or control primary osteocyte-enriched fractions was diluted 1:1 in culture medium.

Osteocyte isolation. Primary osteocyte-enriched fractions from *Men1*^{gtRosaCreERT2} mice were isolated as previously described.[27] Osteocytes were extracted by sequential digestions with collagenase and EDTA (AppliChem, Darmstadt, Germany). Fractions 3–5 of the sequential digest were considered as osteoblasts. Fractions 7–9 and cells derived from bone particles were pooled and considered as osteocytes. After one passage, 8000 cells per well were seeded into collagen-coated 96-well plates (Greiner Bio-One, Kremsmünster, Austria) and treated with 1 μM 4-OHT for 3 days.

Co-culture experiments. BMCs were isolated from wild-type mice and 200 000 cells per well were added on top of primary osteocyte-enriched fractions or primary osteoblasts cultivated in co-culture medium (α-MEM supplemented with 10 nM 1,25-dihydroxyvitamin D3 (Sigma-Aldrich) and 20 ng/ml M-CSF). For pit assay, bone slices (Immunodiagnostic Systems, Tyne and Wear, UK) were used. Cells were removed from bone slices with 1 M ammonium hydroxide overnight and the resorption pits were visualized using 0.5% (w/v in H_2O) toluidine blue.

For conditioned medium-transfer experiments, conditioned medium from *Men1*-deficient primary osteocyte-enriched fractions or control primary osteocyte-enriched fractions was diluted 1:1 in co-culture medium.

For neutralizing antibody experiments, CXCL10-neutralizing antibody (20 ng/ml; R&D Systems) or IgG was added to co-cultures of wild-type BMCs with *Men1*-deficient primary osteocyte-enriched fractions in co-culture medium.

The medium was changed every 3 days. After 9 days, cells were stained for TRAP activity.

Sorting of GFP+ primary osteocytes from Men1^{Dmp1Cre} × Rosa$^{mT/mG}$ mice. Primary osteocyte-enriched fractions were isolated from heterozygous (*Men1* flox/+) or homozygous (*Men1* flox/flox) *Men1*^{Dmp1Cre}; Rosa$^{mT/mG}$ mice, and GFP+ cells were sorted using a FACS LSR II and FACSAria II (BD Biosciences, San Jose, CA, USA). GFP+ cells were used for RNA isolation (see below).

Calvarium *ex vivo* culture. *Ex vivo* organ culture from neonatal mouse calvaria was performed as previously described.[28,29] Bone explants from calvaria were obtained by dissecting parietal bones and frontal bones from 7-day-old *Men1*^{flox} or *Men1*^{Dmp1Cre} mice. Calvaria were cut through the sagittal suture and each half was cultured in one well of a 24-well plate. Calvarial halves were treated with 1 μM indomethacin (Sigma-Aldrich) in α-MEM supplemented with fatty acid-free serum albumin (Sigma-Aldrich). After overnight incubation, calvarial halves were treated with CXCL10-neutralizing antibody (20 ng/ml) or IgG in α-MEM supplemented with 10 nM 1,25-dihydroxyvitamin D3 for 5 days. Medium was collected for CTX enzyme-linked immunosorbent assay (ELISA) and calvarial halves were used for RNA isolation or histology.

CXCL10-neutralizing antibody injection *in vivo*. Mouse CXCL10-neutralizing antibody (R&D Systems) or IgG (R&D Systems) was delivered in the space between the subcutaneous tissue and the periosteum over the sagittal suture of the skull. Before the injection, all animals were anesthetized. One dose of CXCL10-neutralizing antibody (100 μg/mouse) or IgG (100 μg/mouse), each in a 100 μl volume, was injected subcutaneously. Mice were killed 5 days after the injection.

RNA isolation and QRT-PCR. Calvaria from 3-day-old mice were immersed in RLT buffer (Qiagen, Hilden, Germany) and subsequently homogenized using a Precellys 24 homogenizer (Peqlab, Erlangen, Germany). After centrifugation for 3 min at 10 000 × *g* at 4 °C, the supernatant was used for total RNA isolation using RNeasy kit according to the manufacturer's instructions (Qiagen).

Primary osteoblasts or primary osteocyte-enriched fractions were lysed and total RNA was isolated (Qiagen). RNA was reverse-transcribed by a cDNA kit (Applied Biosystems, Carlsbad, CA, USA) and real-time qPCR was performed as previously described.[30] Primer sequences are available upon request.

Immunoblotting. Primary osteoblasts stimulated with either hBMP2 (100 ng/ml) or hTGFβ1 (1 ng/ml; PeproTech) following starvation in serum-free medium for 6 h were lysed in lysis buffer (Cell Signaling Technology, Danvers, MA, USA) containing proteinase inhibitor (Roche). Vertebra samples (L5) were pulverized using a mortar and pestle, and suspended in the lysis buffer. Total protein amount was determined by BCA assay (Pierce, Waltham, MA, USA) and immunoblotting was performed with antibodies against pSmad1/5/8 (1:1000; #9511s, Cell Signaling Technology), Smad1/5/8 (1:1000; sc-6031, Santa Cruz Biotechnology, Dallas, TX, USA), pSmad3 (1:1000; #9520, Cell Signaling Technology), Smad3 (1:1000; #9523, Cell Signaling Technology), menin (1:10 000; A300-105A, Bethyl Laboratories, Montgomery, TX, USA), and β-actin (1:1000; sc-1616, Santa Cruz Biotechnology). Band intensity was analyzed using ImageJ software (NIH, Bethesda, MD, USA).

Enzyme-linked immunosorbent assay. Blood was collected into heparin-coated tubes (Sarstedt, Nümbrecht, Germany) and kept at room temperature for at least 30 min before centrifugation at 2000 × *g* at room temperature for 10 min and isolation of the supernatant. PINP ELISA (Immunodiagnostic Systems) were performed with serum, and CTX ELISA (Immunodiagnostic Systems) was performed with serum and conditioned medium, according to the instructions of the manufacturers.

Immunohistochemistry. Paraffin sections (5 μm thickness) of decalcified femurs were subjected to immunohistochemistry as previously described.[13,31] Antigen retrieval was performed with antigen unmasking solution (Vector Laboratories, Peterborough, UK) at 95 °C for 10 min and immunohistochemistry was performed with an antibody against menin (1:3000; A300-105A, Bethyl Laboratories) and a biotinylated secondary antibody (1:200; Vector Laboratories).

Immunofluorescent staining. Cryosections (100 μm thickness) of decalcified femurs were subjected to immunohistochemistry as described elsewhere.[32] Osteocalcin antibody (1:1000; LifeSpan BioSciences, Inc., Seattle, WA, USA) and Alexa Fluor 647 secondary antibody (1:200; Thermo Fisher Scientific, Waltham, MA, USA) were used. A Leica TCS-SP8 confocal microscope with an inverted stand (DMi8) and LAS X Software were used for imaging (Leica, Wetzlar, Germany). Images were taken at 40-fold magnification using a Leica HCX PL FL L 40 × /0.60 objective.

Men1 overexpression in MLO-Y4 osteocyte cell line. RIKEN full-length *Mus musculus Men1* cDNA (F630025E01, Source BioScience, Nottingham, UK) was cloned into a modified lentiviral pLVX-IRES-GFP vector (Clontech Laboratories, Mountain View, CA, USA). The pLVX-IRES-*Men1*-GFP vector or pLVX-IRES-empty-GFP vector was co-transfected with psPax2 vector and pMD2.G vector into LentiX HEK 293T cells using CalPhos Mammalian Transfection Kit (Clontech Laboratories). Lentiviruses were collected and the MLO-Y4 osteocyte cell line was transduced according to the manufacturer's instructions. At 5 days after transduction, the GFP-expressing cells were sorted using a BD FACSARIA III (BD Biosciences) and expanded for further experiments.

Microarray analysis. Total RNAs isolated from primary osteocyte-enriched fractions (80 ng) were processed and labeled for array hybridization using the Ambion WT Expression Kit (Life Technologies, Carlsbad, CA, USA) at the Genomics Core Facility, EMBL Heidelberg, Germany. Labeled, fragmented cDNA (Affymetrix GeneChip WT Terminal Labeling and Controls Kit, Santa Clara, CA, USA) was hybridized to Mouse Gene 2.0 arrays for 16 h at 45 °C (Affymetrix GeneChip Hybridization, Wash, and Stain Kit). Arrays were washed and stained using the Affymetrix Fluidics Station 450, and scanned using the GeneArray Scanner 3000 7G (Affymetrix). Data analysis was performed with software Expression Console (Affymetrix). The estimated probe signals were normalized using the 'Robust Multi-array Average' method, and the expression levels of probe sets were generated in log2 scale that were then assigned to the annotated gene data (41 346 gene data sets). Probe sets with high expression levels ($>$50% of the total probe signals) were selected (19 854 gene data sets). These were submitted to DAVID Bioinformatics Resources (NIH) and annotated secreted factors were identified (775 gene data sets). Fold change values were defined as $2^{\text{expression levels (KO-WT)}}$. Probe sets with fold change values of >1.4 (30 gene data sets) or <0.7 (81 gene data sets) were selected as possible candidate genes for further validation.

Statistical analysis. Data are presented as mean ± standard errors (S.E.M.). Statistical evaluations of two group comparisons were performed using Student's *t*-test. Statistical evaluations of experiments with more than two groups were performed using one-way analysis of variance (ANOVA).

Conflict of Interest

The authors declare no conflict of interest.

Acknowledgements. We are grateful to the staff of the animal facilities of the University of Ulm, led by Dr Petra Kirsch and in particular to Tobias Rappold. We thank Jelena Pistolic and Dr Vladimir Benes from the Genomics Core Facility, EMBL Heidelberg. We thank Dr. Lynda Bonewald for providing MLO-Y4 cells. We also thank Carmen Hamp and Christina Grimm for assistance in expression studies, and Susanne Schmidt for technical assistance. This study was supported by the Boehringer Ingelheim Foundation (to JPT), Deutsche Forschungsgemeinschaft (DFG, Priority Program Immunobone 1468, Tu 220/6-1, 6-2, Collaborative Research Center 1149, C02/INST 40/492-1, Trilateral Consortium Tu 220/12-1 to JPT), and Leibniz Graduate School on Aging, Fritz Lipmann Institute Jena (to SL).

Author contributions

PL, SL, JK, AR, SO, JL, NM, MMZ, MN, RW and MR performed experiments, analyzed data, and contributed to the preparation of the manuscript. UHL, J-PD, PB, CXZ, and JPT analyzed data and contributed to the preparation of the manuscript.

1. Xiong J, Onal M, Jilka RL, Weinstein RS, Manolagas SC, O'Brien CA. Matrix-embedded cells control osteoclast formation. *Nat Med* 2011; **17**: 1235–U1262.
2. Nakashima T, Hayashi M, Fukunaga T, Kurata K, Oh-hora M, Feng JQ *et al.* Evidence for osteocyte regulation of bone homeostasis through RANKL expression. *Nat Med* 2011; **17**: 1231–1234.
3. Dallas SL, Prideaux M, Bonewald LF. The osteocyte: an endocrine cell ... and more. *Endocr Rev* 2013; **34**: 658–690.

4. Ben-awadh AN, Delgado-Calle J, Tu X, Kuhlenschmidt K, Allen MR, Plotkin LI *et al.* Parathyroid hormone receptor signaling induces bone resorption in the adult skeleton by directly regulating the RANKL gene in osteocytes. *Endocrinology* 2014; **155**: 2797–2809.
5. Wijenayaka AR, Kogawa M, Lim HP, Bonewald LF, Findlay DM, Atkins GJ. Sclerostin stimulates osteocyte support of osteoclast activity by a RANKL-dependent pathway. *PLoS One* 2011; **6**: e25900.
6. Yang J, Shah R, Robling AG, Templeton E, Yang H, Tracey KJ *et al.* HMGB1 is a bone-active cytokine. *J Cell Physiol* 2008; **214**: 730–739.
7. Kanazawa I, Canaff L, Abi Rafeh J, Angrula A, Li J, Riddle RC *et al.* Osteoblast menin regulates bone mass *in vivo*. *J Biol Chem* 2015; **290**: 3910–3924.
8. Aziz A, Miyake T, Engleka KA, Epstein JA, McDermott JC. Menin expression modulates mesenchymal cell commitment to the myogenic and osteogenic lineages. *Dev Biol* 2009; **332**: 116–130.
9. Dreijerink KMA, Varier RA, van Beekum O, Jeninga EH, Hoppener JWM, Lips CJM *et al.* The multiple endocrine neoplasia type 1 (MEN1) tumor suppressor regulates peroxisome proliferator-activated receptor gamma-dependent adipocyte differentiation. *Mol Cell Biol* 2009; **29**: 5060–5069.
10. Hendy GN, Kaji H, Sowa H, Lebrun JJ, Canaff L. Menin and TGF-beta superfamily member signaling via the smad pathway in pituitary, parathyroid and osteoblast. *Horm Metab Res* 2005; **37**: 375–379.
11. Sowa H, Kaji H, Hendy GN, Canaff L, Komori T, Sugimoto T *et al.* Menin is required for bone morphogenetic protein 2- and transforming growth factor beta-regulated osteoblastic differentiation through interaction with Smads and Runx2. *J Biol Chem* 2004; **279**: 40267–40275.
12. Sowa H, Kaji H, Canaff L, Hendy GN, Tsukamoto T, Yamaguchi T *et al.* Inactivation of menin, the product of the multiple endocrine neoplasia type 1 gene, inhibits the commitment of multipotential mesenchymal stem cells into the osteoblast lineage. *J Biol Chem* 2003; **278**: 21058–21069.
13. Bertolino P, Tong WM, Herrera PL, Casse H, Zhang CX, Wang ZQ. Pancreatic beta-cell-specific ablation of the multiple endocrine neoplasia type 1 (MEN1) gene causes full penetrance of insulinoma development in mice. *Cancer Res* 2003; **63**: 4836–4841.
14. Rauch A, Seitz S, Baschant U, Schilling AF, Illing A, Stride B *et al.* Glucocorticoids suppress bone formation by attenuating osteoblast differentiation via the monomeric glucocorticoid receptor. *Cell Metab* 2010; **11**: 517–531.
15. Muzumdar MD, Tasic B, Miyamichi K, Li L, Luo L. A global double-fluorescent cre reporter mouse. *Genesis* 2007; **45**: 593–605.
16. Clausen BE, Burkhardt C, Reith W, Renkawitz R, Forster I. Conditional gene targeting in macrophages and granulocytes using LysMcre mice. *Transgen Res* 1999; **8**: 265–277.
17. Rodda SJ, McMahon AP. Distinct roles for Hedgehog and canonical Wnt signaling in specification, differentiation and maintenance of osteoblast progenitors. *Development* 2006; **133**: 3231–3244.
18. Lu Y, Xie Y, Zhang S, Dusevich V, Bonewald LF, Feng JQ. DMP1-targeted Cre expression in odontoblasts and osteocytes. *J Dent Res* 2007; **86**: 320–325.
19. Huang DW, Sherman BT, Lempicki RA. Systematic and integrative analysis of large gene lists using DAVID bioinformatics resources. *Nat Protoc* 2009; **4**: 44–57.
20. Lee J-H, Kim H-N, Kim K-O, Jin WJ, Lee S, Kim H-H *et al.* CXCL10 promotes osteolytic bone metastasis by enhancing cancer outgrowth and osteoclastogenesis. *Cancer Res* 2012; **72**: 3175–3186.
21. Kittan NA, Allen RM, Dhaliwal A, Cavassani KA, Schaller M, Gallagher KA *et al.* Cytokine induced phenotypic and epigenetic signatures are key to establishing specific macrophage phenotypes. *PLoS One* 2013; **8**: 15.
22. Yellin M, Paliienko I, Balanescu A, Ter-Vartanian S, Tseluyko V, Xu L-A *et al.* A phase II, randomized, double-blind, placebo-controlled study evaluating the efficacy and safety of MDX-1100, a fully human anti-CXCL10 monoclonal antibody, in combination with methotrexate in patients with rheumatoid arthritis. *Arthritis Rheum* 2012; **64**: 1730–1739.
23. Coutinho FL, Lourenco DM Jr, Toledo RA, Montenegro FLM, Correia-Deur JEM, Toledo SPA. Bone mineral density analysis in patients with primary hyperparathyroidism associated with multiple endocrine neoplasia type 1 after total parathyroidectomy. *Clin Endocrinol* 2010; **72**: 462–468.
24. Dempster DW, Compston JE, Drezner MK, Glorieux FH, Kanis JA, Malluche H *et al.* Standardized nomenclature, symbols, and units for bone histomorphometry: a 2012 update of the report of the ASBMR Histomorphometry Nomenclature Committee. *J Bone Miner Res* 2013; **28**: 1–16.
25. Parfitt AM, Drezner MK, Glorieux FH, Kanis JA, Malluche H, Meunier PJ *et al.* Bone histomorphometry: standardization of nomenclature, symbols, and units. *J Bone Miner Res* 1987; **2**: 595–610.
26. Amling M, Priemel M, Holzmann T, Chapin K, Rueger JM, Baron R *et al.* Rescue of the skeletal phenotype of vitamin D receptor-ablated mice in the setting of normal mineral ion homeostasis: formal histomorphometric and biomechanical analyses. *Endocrinology* 1999; **140**: 4982–4987.
27. Stern AR, Stern MM, Van Dyke ME, Jaehn K, Prideaux M, Bonewald LF. Isolation and culture of primary osteocytes from the long bones of skeletally mature and aged mice. *Biotechniques* 2012; **52**: 361–373.
28. Ljunggren O, Ransjo M, Lerner UH. *In vitro* studies on bone resorption in neonatal mouse calvariae using a modified dissection technique giving four samples of bone from each calvaria. *J Bone Miner Res* 1991; **6**: 543–550.
29. Lerner UH. Modifications of the mouse calvarial technique improve the responsiveness to stimulators of bone resorption. *J Bone Miner Res* 1987; **2**: 375–383.
30. Tuckermann JP, Kleiman A, Moriggl R, Spanbroek R, Neumann A, Illing A *et al.* Macrophages and neutrophils are the targets for immune suppression by glucocorticoids in contact allergy. *J Clin Invest* 2007; **117**: 1381–1390.
31. Bertolino P, Radovanovic I, Casse H, Aguzzi A,Wang ZQ, Zhang CX. Genetic ablation of the tumor suppresor menin causes lethality at mid-gestation with defects in multiple organs. *Mech Develop* 2003; **120**: 549–560.
32. Ramasamy SK, Kusumbe AP, Wang L, Adams RH. Endothelial Notch activity promotes angiogenesis and osteogenesis in bone. *Nature* 2014; **507**: 376–380.

Supplementary Information accompanies this paper on Cell Death and Differentiation website (http://www.nature.com/cdd)